Available online at www.sciencedirect.com
SCIENCE DIRECT®
ELSEVIER
Journal of Nuclear Materials 322 (2003) 45–56
journal of nuclear materials
www.elsevier.com/locate/jnucmat

A critical examination of the thermodynamics of water adsorption on actinide oxide surfaces

M.T. Paffett [a,*], Dan Kelly [a], S.A. Joyce [a], John Morris [b], Kirk Veirs [c]

[a] Chemistry Division, Los Alamos National Laboratory, MS J964, P.O. Box 1663, Los Alamos, NM 87545, USA
[b] Engineering Science and Applications Division, Los Alamos National Laboratory, Los Alamos, NM 87545, USA
[c] Nuclear Materials Technology Division, Los Alamos National Laboratory, Los Alamos, NM 87545, USA

Received 21 January 2003; accepted 16 June 2003

Abstract

The reversible adsorption of water from actinide oxide surfaces is examined from several viewpoints in this article. A reinterpretation and critical look at the previously published thermodynamic values for desorption of water from PuO_2 [J. Phys. Chem. 77 (1973) 581] are reexamined in light of more recent mathematical treatments of thermal desorption data from high surface area materials. In addition, the time and temperature dependent process of water adsorption/desorption in closed system experiments is examined using chemical kinetics modeling. A simple experimental method and mathematical treatment of determining adsorption enthalpies based upon a closed system is also described. The desorption enthalpy for reversibly adsorbed water from PuO_2 is determined to be a function of adsorbate coverage with values ranging from 51 to 44 kJ mol^{-1} for coverages of one to several monolayers (MLs). Consistent desorption enthalpy values are obtained using either approach thus highlighting the importance of proper interpretation of adsorption parameters determined from high surface area powders. Reversible adsorption/desorption equilibrium of water with actinide oxide materials is discussed from the practical standpoint of storage and subsequent pressurization of containers. These results obtained from PuO_2 surfaces are consistent with desorption enthalpies of water from a low surface area UO_2 that has been measured using ultra-high vacuum thermal desorption mass spectroscopy to be 42.2 kJ mol^{-1}.

1. Introduction

The Department of Energy/Environmental Management (DOE/EM) is responsible for the management and long-term disposition of a variety of materials located at Rocky Flats, Hanford, Savannah River, and other DOE sites. DOE standard 3013-2000, for stabilization, packaging and storage of pure and impure actinide materials, requires thermal stabilization of materials using calcination in air followed by sealing the material in nested welded stainless steel containers prior to storage or transport [1]. The 3013 standard contains an equation that predicts the maximum total pressure build-up in the container over the anticipated storage time of 50 years. The contributors to pressurization (in this equation) arise mainly from decomposition of adsorbed water contained in and on the surface of the hygroscopic PuO_2 and impurity materials, with minor contributions from increases in storage temperature and radiolytic He gas in growth. This equation is designed to describe a worst-case scenario in which the entirety of adsorbed water is converted to gas, and is formulated to insure that pressures will not exceed the strength of the container at the end of 50 years. As a result, concerns about pressure generation rates and absolute pressures in the storage cans have been raised with regard to rupture and dispersal of nuclear materials [2]. Similar issues involving

* Corresponding author. Tel.: +1-505-665-2395; fax: +1-505-665-2342.
E-mail address: mtp@lanl.gov (M.T. Paffett).

0022-3115/$ - see front matter © 2003 Elsevier B.V. All rights reserved.
doi:10.1016/S0022-3115(03)00315-5

H_2 content and total pressure are of concern with respect to the transportation of these materials around the DOE complex.

A key variable in defining storage standards for actinide oxide materials is the amount of residual water remaining in these materials following calcining operations and prior to enclosure of the materials in storage vessels. The amount of adsorbed water present in these scenarios is a crucial element in design considerations because of the pressure build-up arising from vaporization of adsorbed water and other chemical steps (hydroxyl recombination) leading to water desorption and volatilization. In addition, radiolytic processes leading to hydrogen gas generation are also of concern and constitute active areas of study. To design safe storage environments for these materials the bounding thermodynamic constraints must be known with some certainty. In modeling pressurization and hydrogen gas generation events, frequent reference has made to a number of studies where the thermal desorption of water vapor from PuO_2 has been analyzed to derive thermodynamic values [3,4]. In reviewing this literature base several potential errors have been noted that lead to erroneous thermodynamic values needed for safely predicting temperature–pressure regimes of concern for storage conditions. In this work we reexamine this previous literature base for thermal desorption of water from actinide oxides and comment on its validity in modeling efforts. Specific mention of the intrinsic problem of adsorbate readsorption in determining thermodynamic values from thermal desorption data from moderate surface area oxide samples is briefly mentioned and referenced. In addition, we present another simpler method of experimentally determining desorption enthalpies using a closed experimental system configuration. Finally, we present and compare thermodynamic values for desorption of water from planar, monolithic UO_2 using conventional means (e.g., thermal desorption mass spectroscopy) with values determined from PuO_2 solids that do not suffer from mass transfer, readsorption, and other systematic limitations.

2. Experimental

The simulation of thermal desorption spectra was accomplished using several computer programs previously described in [5]. One specific case performs a simple Redhead analysis [6] of desorption peak temperatures to derive an activation energy for desorption assuming a reaction order and pre-exponential value. The second type of program computes a thermal desorption spectrum using a Runge–Kutta routine to solve the Polanyi–Wigner rate expression. This routine can be run using a coverage dependent E_{des} although this was not used here. Examples of the use of this program appear in [6]. The adsorption/desorption behavior of water on surfaces in both sealed and vacuum systems was also modeled using the Chemkin Collection of software by Reaction Design [7], as explained below.

For determining the energetics of water adsorption/desorption from high surface area solids at elevated temperatures, a stainless steel container sealed with a 33.8 mm Conflat© flange was constructed. Three type-K thermocouples were used to determine the temperatures in the container. A 1.034 MPa pressure transducer (Omega Engineering) rated for use to 573 K was threaded into the top flange. A small cup, in which micro-liter aliquots of water were deposited, was held in the headspace above the material. The internal volume was 0.0256 l. Pressure and temperature data were recorded in an ASCII file at 10 s intervals using a LabView© program and National Instruments data acquisition hardware. The container was placed in a copper block machined for a snug fit and wrapped with insulation. Two cartridge heaters controlled by a PID controller were used to heat the copper block, which attained a maximum temperature between 528 and 538 K in approximately 1800 s with a 0.025 kg sample and 3000 s with a 0.050 kg sample. After reaching the maximum temperature, the heaters were turned off and the system cooled back to room temperature in approximately 6 and 9 h for the 0.025 and 0.050 kg samples, respectively. This thermal cycle was used in all experiments.

The plutonium oxide powder was obtained from Department of Energy Materials Identification and Surveillance (MIS) Program. The oxide powder was originally produced at Hanford. Relevant material properties are given in Table 1. Experiments were carried out with 0.025 and 0.050 kg charges of plutonium

Table 1
Material properties of plutonium oxide powder

Date produced	1985
Pu	86 wt%
Total impurities	1.2 wt%
Isotopic distribution	
% ^{238}Pu	0.009
% ^{239}Pu	94.0731
% ^{240}Pu	5.7764
% ^{241}Pu	0.1198
% ^{242}Pu	0.0217
SSA	800 $m^2\,kg^{-1}$
Mean particle size	14 μm

Isotopic distribution data referenced to production date. Material was calcined to 1223 K prior to use and all other properties were determined after calcinations.

oxide powder. The powder was initially dried by thermal cycling the sample container open to a dry, argon atmosphere. When the container was cool enough to handle safely (≈323 K) the lid was bolted on. A thermal cycle with the material verified that the sample was dry as indicated by the absence of pressurization other than expected from ideal gas behavior of initial headspace gas. Typically 25 μl aliquots of water were added to the cup and one or more thermal cycles were run. Thereafter, additional μl water aliquots were added followed by thermal cycling. The container was open less than 5 min for each addition of water. System performance is described later in the results section.

Ultra-high vacuum (UHV) experiments were performed in a chamber with instrumentation for X-ray photoelectron spectroscopy (XPS) and thermal desorption mass spectrometry (TDMS) measurements. TDMS experiments were performed with a 3 $K\,s^{-1}$ ramp rate, with selected mass monitoring using a quadrupole mass spectrometer. The polycrystalline uranium sample was mechanically polished to a mirror finish. Purity of the bulk uranium was 99.97% with the major impurity being C at 300 ppm. Tantalum wires (0.25 mm dia.) were spot-welded to opposite ends of the sample and this assembly was mounted on a holder that permitted resistive heating and liquid nitrogen cooling to a base temperature of 90 K. Temperatures were measured using a type-K thermocouple spot-welded to the edge of the uranium foil. Sample cleaning was achieved by sputtering with 5 keV Xe^+ ions at alternate hot (800 K) and cold (298 K) temperatures (24 h total) until no trace of oxygen or carbon could be detected by XPS. A thin layer (50 nm) of uranium dioxide was prepared atop the uranium metal by a procedure described previously [8]. The D_2O (99% D, Cambridge Isotope Laboratories, Inc.) used in this study was degassed by multiple freeze–pump–thaw cycles. Isotopically enriched oxygen ($^{18}O_2$, enrichment of 99.5%) was purchased from Cambridge Isotopes and used without further purification. Exposures were performed at $T < 100$ K. A directional gas doser of conventional design [9] was used in this study with an enhancement factor of approximately 100 and all exposures are reported using the enhancement.

3. Results

3.1. H_2O thermal desorption review from PuO_2

Frequent reference is made to thermodynamic values derived in [3] in which the thermal desorption of water from PuO_2 was determined using a convention widely adopted in the catalysis literature. The kinetic analysis in [3] determines the activation energy of desorption from the slope of plots where a function incorporating the peak desorption temperature ($2\ln T_m - \ln\beta$; β is the temperature ramp rate) is plotted versus inverse temperature. It is assumed that the reversible adsorption of water is a non-activated process and therefore the enthalpy of adsorption is equal to the activation energy for desorption. For the conditions used in the cited study [3] and those described in later portions of this work this is a valid assumption. In reviewing this data it became apparent that the thermodynamic values ascribed to reversible water desorption from PuO_2 were significantly higher than that seen from other metal oxide surfaces (including UO_2) [10–12]. In addition, the higher temperature process ascribed to second order associative recombination of surface hydroxyls to produce water vapor yielded a thermodynamic value for water desorption that was nearly twice the value observed in other systems (including surface hydroxyl recombination on uranium [10]). These unusually high values provided the impetus to reexamine the data treatment and see if there was any rational reason for this discrepancy.

In Table 2 we list the temperature of the thermal desorption peak maxima (T_m) and activation energies derived in [3] using the aforementioned kinetic analysis. In addition, we list activation energies of reversible water desorption derived from a Redhead analysis [5,6] of desorption peak temperatures, knowledge of the sample heating rate, and an assumed pre-exponential value of 1×10^{13} s^{-1}. Implicit in this analysis is the assumption that the system pumping speed was essentially infinite and that the process can be described reasonably well using a first order kinetic treatment. Readsorption effects at high surface area powders and secondary

Table 2
Peak temperatures and activation energies for water desorption (^1T_m) and hydroxyl recombinative desorption (^2T_m) from PuO_2

Run	^1T_m (K)	β	Literature analysis ($kJ\,mol^{-1}$)	Redhead analysis[a] ($kJ\,mol^{-1}$)	^2T_m (K)	Literature analysis ($kJ\,mol^{-1}$)	Redhead analysis[b] ($kJ\,mol^{-1}$)
FD-A	371	0.073	84.5	107.5	598	284	175.7
FD-B	378	0.161	84.1	107.5	601	284	172.8
FD-C	393	0.363	84.5	108.8	613	284	172.4
FD-D	398	0.498	84.5	109.2	618	284	172.4

[a] Assuming a pre-exponential value of 1×10^{13} s^{-1}.
[b] Assuming a pre-exponential value of 1×10^{-6} m^2 $molecules^{-1}$ s^{-1}.

effects produced by pumping speed limitations have been noted [6,13] to broaden and extend thermal desorption peak spectra to higher temperatures. Using the aforementioned pre-exponential value for desorption (1×10^{13} s^{-1}) the activation energies determined from data in [3] average 107.9 kJ mol^{-1} for the $^{1}T_{m}$ values. The previous analysis [3] of the reversible desorption of water from PuO_2 surfaces produced values of 84.5 kJ mol^{-1}. For the higher temperature process, denoted as $^{2}T_{m}$ in the table and ascribed to recombination of surface hydroxyls, the reported desorption analysis produces a value of 284 kJ mol^{-1}. Our analysis of the $^{2}T_{m}$ desorption peak temperature using the Redhead formalism produces a value of 172.4 kJ mol^{-1} assuming a second order process and desorption pre-exponential of 1.0×10^{-6} m^2 molecules^{-1} s^{-1}. Note that the pre-exponential value used in [3] was approximately 14 orders of magnitude higher than that normally used in simulation or analysis of simple thermal desorption data for a second order process. Additionally, a first order Redhead analysis of desorption peak temperatures using the standard Redhead method and a first order pre-exponential of 1×10^{13} s^{-1} gives a value of 172.4 kJ mol^{-1}.

In Fig. 1 computed thermal desorption line shapes are shown using the assumed pre-exponential values listed above for the first and second order processes (1×10^{13} s^{-1} and 1.0×10^{-6} m^2 molecules^{-1} s^{-1}, respectively). Of note are the intrinsic line shape differences and the narrower overall line-shape for reversible water desorption from the oxide/hydroxyl covered surface than seen in the experimental data of [3]. An extensive discussion of the differences in line shapes for various different order processes has appeared previously and has been adequately addressed in the literature. The interested reader is specifically referred to [14–16]. Note however, that the experimental full width half maximum for desorption data for H_2O from PuO_2 is approximately 100–125 K (4–5 times larger than that observed in the simulation). This suggests that inter-particle mass transfer and re-adsorption effects may be playing an important role in the observations. Surface heterogeneity is an additional plausible argument for broadened line shapes.

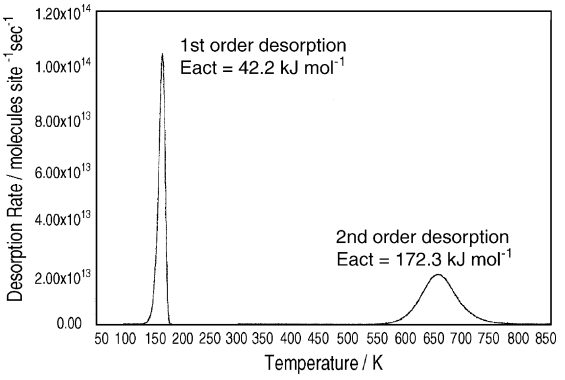

Fig. 1. Simulated thermal desorption peak shapes for a first order and second process with activation energies of 42.3 and 172.4 kJ mol^{-1}, respectively. Assumed pre-exponential values were 1×10^{13} s^{-1} and 1×10^{-6} m^2 molecules^{-1} s^{-1}, respectively.

Numerous references have discussed artifacts and difficulties in extracting kinetic and thermodynamic information from thermal desorption data from porous solids [17–21]. This discussion is not intended to be an exhaustive review on the subject but rather serves as a discourse on how advances in technological and scientific knowledge have altered the validity of some of the previously reported data. In this paper we briefly refer to three such manuscripts that emphasize some of these advanced positions on the importance of instrumental and physical limitations in thermal desorption spectroscopy from porous solids [17–19]. In particular, the work of Hertz et al. [17] and Gorte [18] clearly delineate the effects that concentration gradients, readsorption, mass transfer relating to lag times, and non-infinite pump speed have on thermal desorption profiles. The detailed modeling analysis of Hertz et al. predicts that readsorption effects broaden desorption peaks and can shift them to significantly higher temperature. Gorte demonstrated that readsorption of adsorbates can change thermal desorption peak temperatures by several hundred degrees and these influences cannot be readily eliminated. Both sets of authors clearly state that great care should be taken in interpreting thermal desorption results and that at best only qualitative results should be considered. Pragmatically speaking, desorption temperatures are still of value and qualitative comparisons are still valid. More recent thermal desorption studies, where the amount of porous solid is in the range of micrograms, have been successfully demonstrated by Yates et al. [19]. In this technique, intimate contact of the porous solid with a metal substrate that can be precisely temperature controlled and the elimination of inter-particle contact (reducing mass transfer effects) demonstrate that reasonably well-behaved thermal desorption profiles can be obtained from porous high surface area solids. In these studies the thermal desorption profiles of alkenes from zeolite substrates were obtained with full width of half maximum in the range of tens of degrees. These significantly narrower thermal desorption line width values are in line with the simulation results presented in Fig. 1 above.

3.2. Mathematical modeling description for water adsorption/desorption

As a prelude to data described in the next section water adsorption/desorption phenomena were mathematically modeled using Chemkin modeling software by Reaction Design [7]. Fig. 2 depicts the thermal desorp-

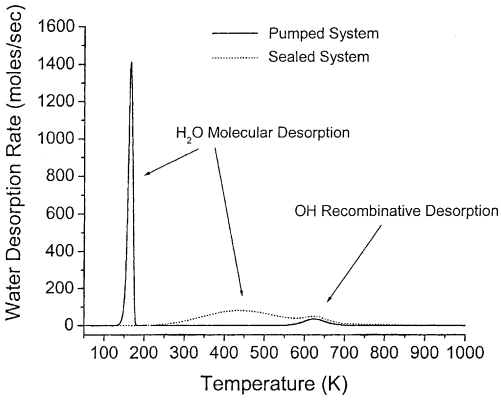

Fig. 2. Simulated thermal desorption of water arising from physically adsorbed water and water created from recombinative desorption of surface hydroxyls from PuO_2 for closed and open systems. The surface was initially covered with 80% H_2O molecules and 20% OH moieties.

tion of water and recombinative desorption of hydroxyls in both sealed and open (well-pumped) scenarios. In this simulation of thermal desorption from a smooth monolithic surface the plutonium oxide was initially covered with 80% H_2O molecules and 20% OH moieties. Using a commonly accepted value of 10^{13} s^{-1} for the pre-exponential value the activation energy fit for H_2O desorption was determined to be 42.3 kJ mol^{-1}. Alternatively a pre-exponential value of 10^{16} s^{-1} can be used in it follows that the desorption enthalpy is determined to be 50 kJ mol^{-1}. The activation energy for recombination of hydroxyls leading to water desorption was fit with 172.4 kJ mol^{-1} and the pre-exponential value was fixed at 10^{-6} m^2 $molecules^{-1}$ s^{-1}. Note the significant difference in the thermal desorption behavior of water molecules in open vs. closed systems. In the open system where effective pumping speeds are large, thus approximating traditional UHV thermal desorption studies, water desorbs at ~165 K in agreement with Fig. 2 as expected. In a closed system however, where the desorbed water remains in proximity to the surface and may readsorb, the thermal desorption feature for molecular water is significantly broadened and peaks at a temperature of ~440 K. Thus, independent of mass transfer or surface heterogeneity effects, the thermal desorption behavior of species in sealed (or poorly pumped) systems are significantly affected by their ability to readsorb.

The water adsorption/desorption experimental data recorded from PuO_2 powder samples of Fig. 5 (described and shown later) was simulated using the Chemkin Aurora application module, which simulates a constant stirred tank reactor. The Aurora module was run in a closed-system transient mode to determine canister pressure as a function of time. In Eq. (1) a simple reaction mechanism is presented which describes desorption and adsorption of water from a PuO_2 surface:

$$H_2O_{(s)}/PuO_2 \Longleftrightarrow H_2O_{(g)} + PuO_2 \quad (1)$$

The kinetics of desorption is typically described by the Polanyi–Wigner rate equation (Eq. (2)) where k_d is the rate coefficient for desorption and E_{des} is the desorption energy for water,

$$k_d = 10^{13}\ s^{-1} * \exp(-E_{des}/RT), \quad (2)$$

which varies with coverage as further explained below. Chemkin allows for the incorporation of coverage dependent reaction rate parameters. (Since the relatively small mass loadings of water in Section 3.3 correspond to multiple layers of adsorbed water on PuO_2, the ability to incorporate concentration-dependent water reactions into the model may be paramount to proper description of the overall system behavior.) While a single sticking coefficient and a single desorption energy used in Eq. (1) above are sufficient to reproduce the peak pressures observed experimentally for all water loadings, the functionality of the higher water loading curves exhibited with surface temperature, T_s, is not captured without coverage dependent rate parameters. The sticking probability was varied linearly with increasing water loading from $S = 0.07$ on the bare PuO_2 surface to $S = 1$ at 0.18 wt% loading. A reaction probability for water adsorption on bare UO_2 has been reported from which S has been inferred to be 0.07 [22], and multiple workers have found the sticking probability of water on water to be equal to unity [22–24]. It may well be that the sticking probability of water approaches unity with increasing water coverage more rapidly (and maybe non-linearly) than with a linear function. A value of unity for the sticking coefficient at a loading of 0.18 wt% was chosen because this is the maximum amount of water used in the experiments of Section 3.3. While 0.18 wt% of water corresponds to approximately 7.5 ML of water (see below), it is not anticipated that water will adsorb in a layer-by-layer fashion based upon the heterogeneous nature of the oxide surface and other factors [12]. Hence the overall sticking probability will not simply vary linearly from $S = 0.07$ on the bare PuO_2 to $S = 1$ when a single monolayer equivalent of water is adsorbed. Also of note is that sticking probabilities are generally not strongly dependent upon T_s, and therefore the sticking probability is assumed to be independent of T_s in the simulations. Analyses of Figs. 5 and 6 (see Table 3) indicate that approximately 2 ML equivalents of water adsorb with a constant heat of adsorption that is slightly higher than the heat of vaporization of water (averaging ~50 kJ mol^{-1} in the analysis vs. 44 kJ mol^{-1} for ΔH_{vap}). We therefore set $E_d = 50$ kJ mol^{-1} at all T_s for the 2 ML equivalents of water nearest the PuO_2 surface. The remaining water desorbs with $E_d = \Delta H_{vap}$, where ΔH_{vap} is dependent on surface temperature and varies from approximately 43.990 kJ mol^{-1} at $T_s = 300$ K to

Table 3
Results of a fit to the data using Eqs. (4) and (5)

Run	n_m kg of H_2O per kg of PuO_2 ($\times 10^{-3}$)	ΔH_{ads} kJ mol^{-1}	T (K)	n_{tot} kg of H_2O ($\times 10^{-6}$)
004	0.16	−6.32	461	45
005	0.17	−5.31	461	43
006	0.16	−5.73	483	64
007	0.19	−4.77	483	62
008	0.18	−5	498	82
009	0.19	−5.01	498	81
010	0.19	−5.17	498	80
012	0.19	−4.81	498	78
013	0.19	−4.36	498	77
014	0.19	−4.98	498	77
019	0.19	−5.85	426	23
020	0.23	−4.54	426	23
021	0.22	−5.27	426	23
022	0.23	−4.63	425	22.5
023	0.23	−6.12	465	48
024	0.23	−5.55	465	47.5
025	0.22	−5.9	464	47
026	0.23	−5.26	464	46.5
027	0.21	−5.68	489	71
028	0.2	−6.09	488	70
029	0.22	−5.7	488	70
031	0.18	−6.55	506	92
032	0.22	−5.74	506	92.5
033	0.24	−5.56	506	93
034	0.21	−5.34	505	91
Average	0.2028	−5.4096		
Σ	0.023544285	0.570208		
SSA	920 m^2 kg^{-1}			

The SSA is obtained by dividing the mass of water per kg of PuO_2 by the mass of water in a monolayer taken to be 2.2×10^{-4} kg per monolayer from [29]. The amount of water available is given as n_{tot}.

31.809 kJ mol^{-1} at $T_s = 513$ K [25]. In all cases the pre-exponential factor of Eq. (2) is assumed to be independent of water coverage and surface temperature. Chemkin solves the adsorption/desorption reaction equations to evaluate the overall rate of water adsorption/desorption. This modeling approach determines a specific rate of desorption at a given temperature given specific input such as the PuO_2 surface site density (ρ in mol m^{-2}), the total PuO_2 site area (SA given in m^2), and the amount of adsorbed water [H_2O]. The overall rate is expressed in Eq. (3) as

$$\text{rate} = k_{des} * \rho * SA * [H_2O]. \quad (3)$$

The simulation parameters and methodology used an initial PuO_2 loading of 0.025 kg with a density of 11.5 g cm^{-3}. The oxide has a measured BET surface area of 800 m^2 kg^{-1} and assuming a molecular area for water adsorption of 0.10 nm^2, we note that 0.05 wt% H_2O corresponds to a surface coverage of approximately 2.1 ML of H_2O on 0.025 kg of this oxide sample. The canister is packaged in dry Ar at 7.57×10^4 Pa (ambient pressure in Los Alamos). The time dependent temperature profile of the simulation was set to exactly match that measured experimentally (data not shown). The simulation accounts for changes in canister pressure arising from temperature changes, as expected from the ideal gas law.

Fig. 3 shows the results of the Aurora simulation along with the experimental data of Fig. 5. For clarity, the plots are cast as pressure vs. time rather than pressure vs. temperature (temperature was cycled from 300 to 525 and then back to 325 K). The results of Fig. 3 indicate that our modeling efforts and protocol adequately model the adsorption data of Figs. 5 and 6.

3.3. Water adsorption/desorption on PuO_2 in a closed system

The pressure behavior for a closed system of PuO_2 powder in a sealed container with deliberate addition of water was examined for practical implications. In the process of doing so a critical evaluation of the data

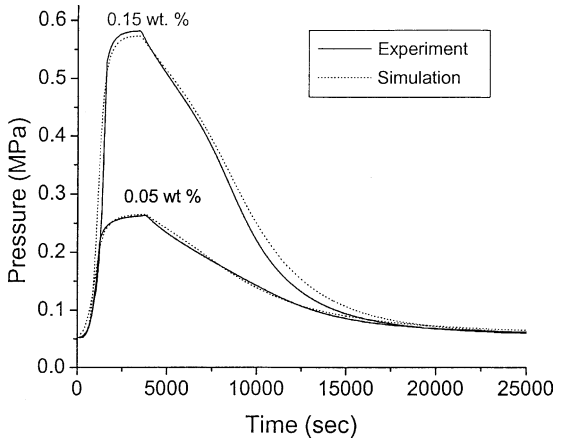

Fig. 3. Simulated vs. experimental measurements of pressure for the data of Fig. 5. For clarity, the plots are cast as a function of time rather than temperature.

revealed that thermodynamic information can be obtained assuming a reversible adsorption/desorption process. Pressure vs. time (or temperature) data for an empty container (minus the PuO_2) was monitored during cool-down with added water and is shown in Fig. 4. The observed data is compared to the vapor pressure of water obtained from the NIST Steam Tables© for saturated vapor (see Appendix A). The agreement between observed and expected behavior is excellent. Following this characterization test six thermal cycles for the 0.050 kg of PuO_2 sample with 100 μl of water added are shown in Fig. 5. A number of important characteristics are apparent. First, during the heating portion, water is desorbed until a plateau is reached and no additional

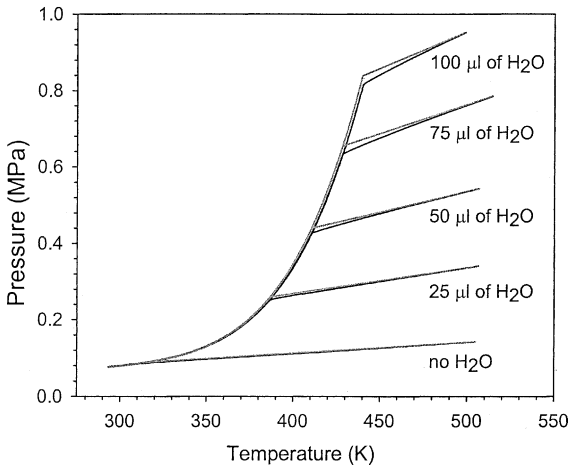

Fig. 4. Pressure in empty, sealed container with varying amounts of water added. The grey lines are predicted values using the NIST Steam Tables and the black lines are the observed data.

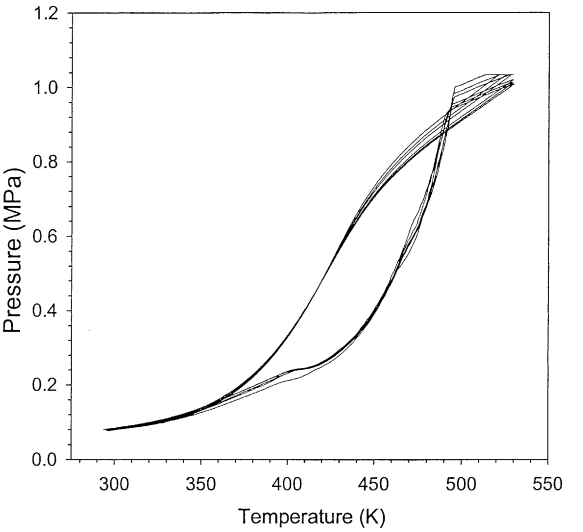

Fig. 5. The pressure response during six consecutive thermal cycles of the container with 0.0494 kg of PuO_2 powder after drying followed by the addition of 100 μl of water.

water is evolved. Further heating results in a linear increase in pressure consistent with thermal heating of an ideal gas. Second, the pressure behavior during the cooling portion of the cycle is significantly different than during the heating cycle. The cooling portion of the cycle is considered to be in equilibrium (maximum temperature differences between the three thermocouples at 473 K are 44 K during heating and 4 K during cooling.) Therefore, only the cooling portion of the thermal cycle is considered further. Small pressure decreases are observed with each thermal cycle (evident from the decreasing pressure plateaus with each cycle) and this behavior is attributed to the slow kinetic corrosion reaction of PuO_2 producing a thickening hydroxide layer on the high surface area powder. This aspect is addressed in a separate publication [26] and is the focus of continuing studies in relation to the role of hydroxide in hyper-stoichiometric PuO_{2+x}.

Fig. 6 shows the pressure vs. temperature for a sealed canister of 25 g PuO_2 loaded with 0.05 and 0.15 wt% H_2O (12.5 and 37.5 μl H_2O, respectively). System temperature was raised from room temperature to 530 K over approximately 30 min and cooled over approximately 6 h. Arrows on the figure indicate the temperature cycle. The data are readily compared with the saturated vapor pressure of water obtained from the NIST Steam Tables. The data obtained during the cool down portion of the ramp was corrected for fill gas pressure contribution and the remaining pressure (attributed to water vapor in equilibrium with the PuO_2 powder) was divided by the saturated vapor pressure of water vapor from the NIST Steam Tables. This ratio is designated as P/P_0 by analogy with a more conventional

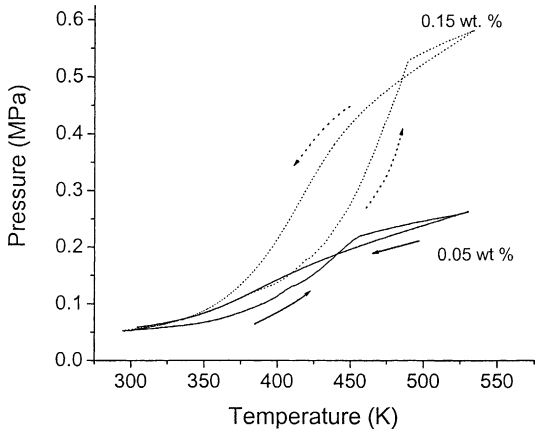

Fig. 6. Pressure vs. temperature for a sealed canister and water loadings of 0.05 and 0.15 wt% (12.5 and 37.5 μl) on 0.025 kg PuO_2. The temperature was raised from room temperature to approximately 533 K, and returned to room temperature as indicated by the arrows.

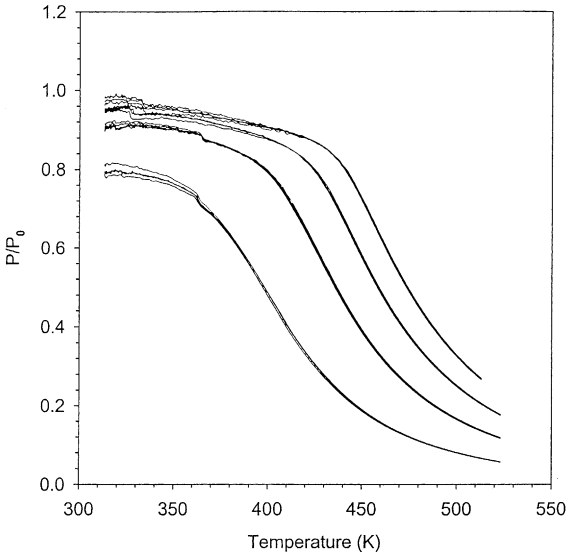

Fig. 7. The vapor pressure of water adsorbed to plutonium oxide powder divided by the saturated vapor pressure of water as a function of temperature. The four sets of curves are for 25, 50, 75, and 100 μl of added water (from top to bottom respectively). The breaks in the curves occurring between 0.7 and 0.9 P/P_0 are seen when less than 3.5 ML equivalents of water remain on the surface. For the 25 μl aliquot of water, the amount of water on the surface is below the 3.5 ML equivalents and therefore does not exhibit a significant break.

BET analysis of surface area from a high surface area solid. Keep in mind that a conventional BET analysis is typically performed at a constant temperature while varying the pressure of a gaseous adsorbent in a systematic manner. Despite this fundamental difference in approach we plot in Fig. 7 P/P_0 as a function of temperature for PuO_2 material with 25, 50, 75, and 100 μl additions of water. At P/P_0 ratios above 0.8, the water is behaving essentially like liquid water. Normally the data plots in Fig. 7 for different water loadings should all approach 1.0 at the low temperature limit. The differences arise from temperature differences within the container (general system performance is such that a 4 K difference is sufficient to reduce the P/P_0 ratio from 1.0 of liquid water to 0.8).

The amount of water remaining on the surface at a given temperature is computed from the total amount of water loaded in the container minus the amount of water in the vapor phase obtained from the ideal gas law, and vapor pressure of the water. The amount of water on the 0.025 kg PuO_2 solid sample is plotted as a function of the P/P_0 ratio in Fig. 8. Although the data was obtained over a range of temperatures, the form of the curves acquired with different mass loadings of water are virtually superimposable and closely resemble a standard type II adsorption isotherm [27]. Note however that the inflection point normally observed at low values of P/P_0 and attributed to a monolayer packing of adsorbate is not seen in the water data obtained from PuO_2 because the data are not available in this case to make an accurate plot. In general the inability to discriminate such a feature is indicative of the fact that small or insignificant differences exist in the adsorption enthalpy between the monolayer and the multilayer adsorption. Despite this limitation we have recast the P/P_0 data (in a manner similar to that performed on true BET data) as a linear

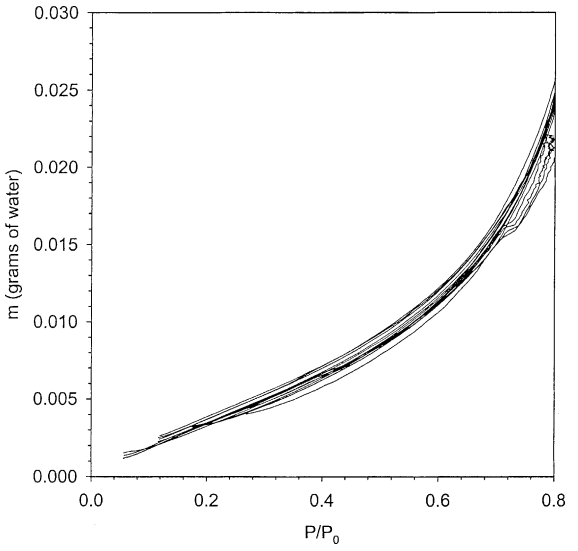

Fig. 8. The amount of water adsorbed on the surface as a function of the relative water vapor pressure. This is equivalent to a standard adsorption isotherm.

function of P/P_0, in which the slope and intercept are related to the amount of adsorbate in a monolayer and the excess heat of adsorption,

$$\text{Slope} = \frac{1}{c \cdot n_m}, \tag{4}$$

where $c = e^{\Delta H_{ads}/RT}$ and n_m is the mass of a monolayer and

$$\text{Intercept} = \frac{(c-1)}{c \cdot n_m}. \tag{5}$$

From the slope and intercept of the data plots c and n_m were evaluated. The results are given in Table 3. The specific surface area (SSA) obtained from this procedure is in excellent agreement with the standard BET nitrogen adsorption SSA of 800 $m^2\,kg^{-1}$ (determined independently). The excess heat of adsorption of water onto plutonium oxide is determined at a temperature where P/P_0 is 0.3 and is 5.4 ± 1.1 $kJ\,mol^{-1}$. Excess enthalpies of water adsorption determined at P/P_0 values of 0.2–0.4 range from 4.3 to 6.8 $kJ\,mol^{-1}$. The power of this technical approach to treating the pressure vs. temperature ramp data obtained from a sealed container lies in the ability to obtain thermodynamic values for water adsorption that are self-consistent with UHV data. Despite the fact that the temperature varies in this experiment the reversibility of the system allows the approach to work. If significant irreversible reactions or other secondary reactions were occurring that would influence the pressure over these time frames the approach would be compromised. In actuality cycling of the PuO_2 powder in the presence of water vapor at the higher temperature regimes ($T > 450$ K in Fig. 5) shows a slight decrease in overall pressure and is attributed to the water-assisted corrosion of PuO_2 and is the focus of another study. Furthermore, the amount of water determined by this approach for a monolayer (whether in weight or $mol\,m^{-2}$) is in surprising good agreement with values determined from model estimates and is self-consistent [28].

4. Discussion

Thermodynamic values for desorption enthalpies from specific surfaces are typically determined using smooth monolithic surfaces in concert with a controlled temperature ramp and sensing instrument (most frequently a mass spectrometer). In general the absolute values for the adsorption and desorption enthalpies should be equivalent unless the adsorption process is activated. In this and other work no indication of an activated adsorption process has ever been noted on either PuO_2 or UO_2. Water interactions with surfaces have been extremely well studied and extensive literature reviews and implications are addressed in [11,12]. With respect to the actinide oxide surfaces a paucity of references on the desorption of water from well-defined actinide single crystals precludes a detailed literature comparison to values obtained from non-actinide surfaces. An exception to this statement is data obtained from UO_2 surfaces. We begin our discussion by examining some critical features of this data.

In Fig. 9 we display the thermal desorption mass spectroscopy traces of water entities following a 4 L exposure of $D_2^{16}O$ onto a previously prepared $U^{18}O_2$ surface. The isotopic distribution of the desorbing water species clearly indicates that residual H atoms in the bulk of the sample migrate and recombine to form odd

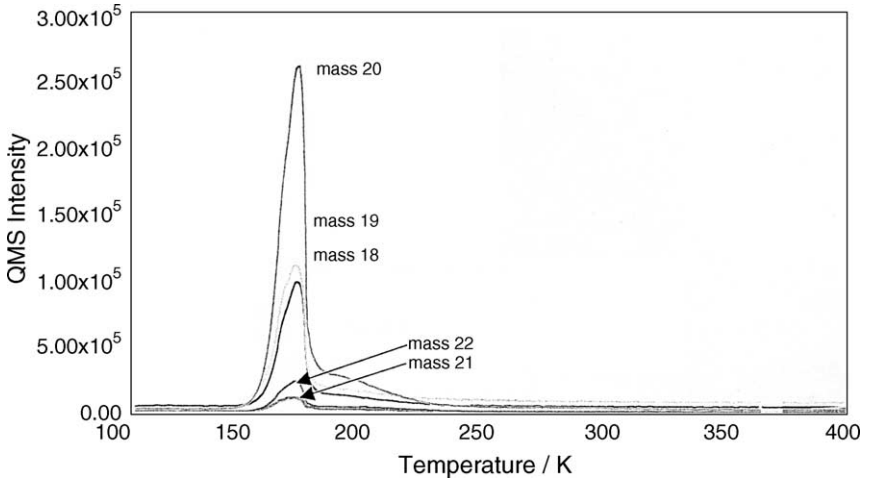

Fig. 9. Multiplexed thermal desorption mass spectra of D_2O from a $U^{18}O_2$ thin film atop U substrate. Initial D_2O exposure was 4 L (5.3×10^{-4} $Pa\,s^{-1}$ = 4×10^{-6} $Torr\,s^{-1}$).

mass fractions ($m/e = 19, 21$; although wall interactions can also contribute to this observation). In addition, the presence of water molecules containing ^{18}OD fragments ($m/e = 21, 22$) clearly indicates that at temperatures below the desorption temperature of water, 170 K, O–H bond scission occurs to some small but observable extent. In other related studies the persistence of low coverages of OH fragments (below photoelectron detection limits of several percent of a monolayer) to temperatures as high as 600 K are observed in electron stimulated desorption of OH^+ fragments following the exposure of D_2O to a $UO_2(1\,0\,0)$ surface [29]. The mechanistic details of these molecular scale events are beyond the scope of this study and will be reported in a separate publication [29]. In addition, the growth and thermal stability of surface hydroxyls have been noted in XPS studies of PuO_2 powders and based upon photoelectron mean free paths the depth of hydroxyls conversion on these PuO_2 solids following realistic water exposure is on the range of 2–4 nm [30].

In the context of this study however, the desorption peaks in Fig. 9 exhibit narrow line shapes consistent with simulated first order desorption processes. Although not shown the experimental line shapes can be fit using a reversible first order desorption activation energy of 42.3 $kJ\,mol^{-1}$ and a pre-exponential factor of 1×10^{13} s^{-1}. These values are in line with water desorption from other metals and metal oxides surfaces and significantly lower than those values previously reported from PuO_2 [3]. On the sum of the data and modeling results obtained from water adsorption/desorption from high surface area PuO_2 powders these values are remarkably consistent and similar. In addition there appears to be nothing unusual in regard to the nature of the PuO_2 surface that would make this thermodynamic value considerably different.

There have been several reports addressing the kinetics of water uptake and equilibrium amounts of water adsorbed onto PuO_2 powders. Of specific mention are the works of Haschke and Ricketts [28] and Benhamou and Beraud [31]. In the thermogravimetric study of Benhamou and Beraoud the effects of calcination temperature of the PuO_2 powder and relative humidity were specifically addressed in the context of equilibrium amounts of water adsorbed as a function of time. Several key features were observed. Namely that for PuO_2 calcined to progressively higher temperatures possessing lower surface areas low amounts of water were adsorbed following exposure to relative humidities in the range of 60%. Equilibrium water adsorption for PuO_2 powder calcined above 873 K amounted to less than 0.5 wt% for relative humidities of 60% or less. Furthermore, the absolute amounts of water adsorbed and behavior observed in a thermogravimetric analysis instrument produced results very similar to those observed in Fig. 8. Whereas the TGA technique specifically measures weight gain (or loss) resulting from adsorbed water, the pressure measurement indicated in our approach indirectly provides complementary information by measuring the water not adsorbed and present in the gas phase. The physical properties of the PuO_2 materials were virtually identical and aside from the higher pre-calcination temperature used in the French work the amount of water adsorbed in specific cases are virtually identical to those seen here. These slight differences are attributed to the participation of the surface hydroxyl entities that are always present on the materials used in the sealed container approach of our study (because of the heating limitation). Regardless of these differences the consistency of the results from both approaches is good.

The more recent article by Haschke and Ricketts [28] addresses the kinetics and equilibrium water adsorption on PuO_2. Several points are worth noting in the work. A consistent treatment and derivation of the specific weight (and hence area) of adsorbed water molecule of 2.2×10^{-7} $kg\,m^{-2}$ is presented and is consistent with the BET analysis of water adsorption in our results. Secondly the kinetics of uptake are examined and although of extreme pragmatic use in actually processing and packaging operation involving PuO_2 powders, these results will be system dependent with respect to mass transfer effects. Again these mass transfer effects have been noted to seriously compromise strict thermodynamic interpretation in the work of Stakebake (previously discussed). Finally the concept of separate and distinct thermodynamic values for desorption of a large number of different water layers from PuO_2 high surface area powders is introduced in [28]. This is somewhat surprising and inconsistent with all known observations of water on other metal oxides (and metals for that matter) [10–12]. Occasionally in studies of water desorption from low surface area monolithic substrates 2 desorption states can be observed but the delineation of 5 separate and distinct interactions involving 10 molecular layers has never been observed on any other oxide surface (as suggested in [28] for PuO_2). From the data presented along with the modeling results one is hard pressed to make a case for more than 1–2 molecular layers of water being distinctly observed and accurately accounted for in interpreting the thermodynamics of adsorption/desorption from PuO_2. In addition, the behavior of water adsorption/desorption from UO_2 is also consistent with this view that although the first monolayer of water may desorb at a ever so slightly higher temperature than multi-layer desorption of water no observation or indication that other layers possessing any unique characteristics that are observable in thermal desorption phenomena. One of the major points that we make in this work is that desorption data from high surface area powders is compromised for use in thermodynamic calculations because of readsorption (mass transfer) effects and that careful consideration should be

given before one interprets or models expected behavior using such data.

Finally, the pragmatic implications concerning the use of correct thermodynamic values for water adsorption/desorption from these high surface area actinide solids have been discussed in several of our recent publications [32,33]. The correct value for water adsorption/desorption indicates that actual pressure considerations for long term storage of PuO_2 powders following 3013 processing conditions and container sealing procedures can be dominated by water vapor in some actual storage scenarios.

5. Conclusions

In summarizing the important contributions of this work we have

(1) reevaluated previous thermal desorption data for water desorbing from PuO_2;
(2) modeled real thermal desorption data using these improved thermodynamic values to produce a self consistent interpretation;
(3) developed a self-consistent simple experimental method of evaluating desorption enthalpies using high surface area powders in a sealed container for reversible systems that are not activated; and
(4) determined that the enthalpy of desorption of water from PuO_2 lies in the range of 44 to 51 kJ mol^{-1} for coverages of one to several monolayers.

These results taken together suggest that the reactions and subsequent thermal chemistry of water on PuO_2 can be described with thermodynamic values that are similar to those seen for other metal oxide surfaces, in particular the UO_2 surfaces. Further work delineating the differences inherent in radiolytically driven surface as well as the water assisted corrosion of PuO_2 chemistry constitute the focus of additional studies.

Acknowledgements

Funding for this investigation was made possible by the Nuclear Materials Stabilization Program Office, United States Department of Energy, Albuquerque Operations and Headquarters Offices, under the auspices of the DNFSB 94-1 Research and Development Project.

Appendix A

In order to compare the observed pressure to NIST calculated water vapor pressures at large numbers of temperatures, an algorithm was developed that could be easily implemented in a modern spreadsheet.

$$P(T) = \frac{[-1 + (1 + 4B'(T)f(T))^{0.5}]}{2B'T}, \quad \text{where } B'T = \frac{B(T)}{RT}, \tag{A.1}$$

$$f(T) = a\mathrm{e}^{-\Delta G^0(T)/RT}, \quad \text{where } a = 1, \tag{A.2}$$

$$\Delta G^0(T) = [H^0_{298} - T\,\Delta\Phi^0(T)], \quad \text{where } \Delta H^0_{298} = 44.004 \text{ kJ mol}^{-1}, \tag{A.3}$$

$$\Delta\Phi^0(T) = \frac{-[G^0 - H^0(T)]}{T}. \tag{A.4}$$

The temperature dependence of the second virial coefficient was obtained from a fit of the tabulated values [34]. This function is

$$B(T) = \frac{0.0015}{1 + \frac{T}{10\,000}} - 0.000942 \times (1 - \mathrm{e}^{-1500/T})^{2.5}\left(\frac{T}{1500}\right)^{0.5}\mathrm{e}^{1500/T} - 0.0004882\frac{1500}{T}. \tag{A.5}$$

The temperature dependence of $\Delta\Phi^0$ was obtained from a fit of values of $\Delta\Phi^0$ at 373, 473, 573, and 673 K taken from the NIST Steam Tables. This function is

$$\Delta\Phi^0(T) = \frac{1}{a + bT^{0.5} + \frac{c}{T}}, \quad \text{where } a = 0.0027611, b = 0.00021827, \text{ and } c = 0.56099. \tag{A.6}$$

This calculation approach yielded saturated vapor pressures of water that agreed with pressures from the NIST Steam Tables to better than 0.2% over the temperature range of 283–523 K.

References

[1] Stabilization, Packaging, and Storage of Plutonium-Bearing Materials, Department of Energy, DOE-STD-3013-2000, September 2000.
[2] Assessment of Plutonium Storage Safety Issues at Department of Energy Facilities, US DOE Report DOE/DP/0123T, US Department of Energy, Washington, DC, 1994.
[3] J.L. Stakebake, J. Phys. Chem. 77 (1973) 581.
[4] J.L. Stakebake, L.M. Steward, J. Colloid Interface Sci. 42 (1973) 328.
[5] M.E. Jones, B.E. Koel, R.T. Weppner, Surf. Sci. 233 (1990) 65.
[6] P. Redhead, Vacuum 12 (1962) 203.
[7] R.J. Kee et al., Chemkin Collection Release 3.6, Reaction Design, Inc., San Diego, CA, 2000.

[8] J.G. Dillard, H. Moers, H. Klewe-Nebenius, G. Kirch, G. Pfennig, H.J. Ache, Surf. Sci. 145 (1984) 62.
[9] C.T. Campbell, S. Valone, J. Vac. Sci. Technol. A 3 (1985) 408.
[10] W.L. Manner, J.A. Lloyd, M.T. Paffett, J. Nucl. Mater. 275 (1999) 37.
[11] P.A. Thiel, T. Madey, Surf. Sci. Rep. 7 (1987) 211.
[12] M. Henderson, Surf. Sci. Rep. 46 (2002) 1.
[13] D.A. King, CRC Crit. Rev. Solid State Mater. Sci. 7 (1978).
[14] J.T. Yates Jr., in: Methods of Experimental Physics, vol. 22, Academic Press, New York, 1985, p. 425.
[15] J.B. Miller, H.R. Siddiqui, S.M. Gates, J.N. Russell Jr., J.T. Yates Jr., J. Chem. Phys. 87 (1987) 6725.
[16] D.H. Parker, M.E. Jones, E. Mark, B.E. Koel, Surf. Sci. 233 (1990) 65.
[17] R. Hertz, J. Kiela, S. Marin, J. Catal. 73 (1982) 66.
[18] R. Gorte, J. Catal. 75 (1982) 164.
[19] P. Basu, J.T. Yates, Surf. Sci. 177 (1986) 291.
[20] J. Rieck, A.T. Bell, J. Catal. 85 (1984) 143.
[21] D. Edwards, Surf. Sci. 49 (1975) 393.
[22] M. Balooch, A.V. Hamza, J. Nucl. Mater. 230 (1996) 259.
[23] D.E. Brown, S.M. George, C. Huang, E.K.L. Wong, K.B. Rider, R.S. Smith, B.D. Kay, J. Phys. Chem. 100 (1996) 4988.
[24] Y.Q. Li, P. Davidovits, Q. Shi, J.T. Jayne, C.E. Kolb, D.R. Worsnop, J. Phys. Chem. 105 (2001) 10627.
[25] K.N. Marsh (Ed.), Recommended Reference Materials for the Realization of Physicochemical Properties, Blackwell, Oxford, 1987.
[26] M.P. Neu, S.D. Conradson, D.W. Keogh, S.D. Reilly, R.K. Schulze, C.D. Tait, J.H. Terry, Abstr. Pap. Am. Chem. Soc. 217 (part 2) (1999) 46.
[27] F. Roquerol, J. Roquerol, K. Sing, Adsorption by Powders and Porous Solids, Academic Press, London, UK, 1999.
[28] J. Haschke, T. Ricketts, J. Alloy Compd. 252 (1997) 148.
[29] S. Joyce, unpublished results, 2002.
[30] J.D. Farr, R.K. Schulze, M. Neu, L. Morales, manuscript submitted 2003.
[31] A. Benhamou, J.P. Beraud, Analusis A 8 (1980) 376.
[32] M. Paffett, D. Kelly, in: American Nuclear Society Topical Conference on Spent Nuclear Fuel and Fissle Materials, Charleston, SC, September 2002, American Nuclear Society Publications, LAUR 02-4349.
[33] D. Kelly, M.T. Paffett, in: Proceedings of Waste Management 2002, Tucson, AZ, February 2002, American Nuclear Society Publications.
[34] E.J. LeFevre, M.R. Nightingale, J.W. Rose, J. Mech. Eng. Sci. 17 (1975) 243.